Supplementary Information for

Swi5-Sfr1 Stimulates Rad51 Recombinase Filament Assembly by Modulating Rad51 Dissociation

Chih-Hao Lu[1], Hsin-Yi Yeh[2], Guan-Chin Su[2], Kentaro Ito[3], Yumiko Kurokawa[3,¶], Hiroshi Iwasaki[3,*], Peter Chi[2,4,*] and Hung-Wen Li[1,*]

[1] Department of Chemistry, National Taiwan University, Taiwan
[2] Institute of Biochemical Sciences, National Taiwan University, Taiwan
[3] Institute of Innovative Research, Tokyo Institute of Technology, Japan
[4] Institute of Biological Chemistry, Academia Sinica, Taiwan

[*] To whom correspondence should be addressed:
Hiroshi Iwasaki, E-mail: hiwasaki@bio.titech.ac.jp
Peter Chi, E-mail: peterhchi@ntu.edu.tw
Hung-Wen Li, E-mail: hwli@ntu.edu.tw
[¶] current address: Center for Frontier Research, National Institute of Genetics, Japan

This PDF file includes:

Supplementary text
SI Materials and Methods
Figures S1 to S11
Tables S1 to S10
References for SI reference citations

Author contributions: C.H.L., H.I., P.C. and H.W.L. designed research; C.H.L. performed all single-molecule experiments and analyzed data; H.Y.Y, G.C.S., K.I. and Y.K. purified proteins used in this article; C.H.L. H.I., P.C. and H.W.L. wrote the paper.

www.pnas.org/cgi/doi/10.1073/pnas.1812753115

SI Materials and Methods

DNA substrates. The $(dT)_{135}$ gapped DNA substrate for TPM assembly and disassembly experiments contains 135 nt poly dT sandwiched by a 151 bp, 5′-digoxigenin-labeled dsDNA handle and a 5′-biotin-labeled 19 bp handle. To prepare the $(dT)_{135}$ gapped DNA, we first used auto-sticky polymerase chain reaction (PCR)(1) to prepare a 131/151 hybrid DNA with a 20 nt 5′-overhang using a digoxigenin-labeled primer (5′-dig/CGTGGGTATGGTGGCAGG), and a primer containing an abasic nucleotide at the 21th position (5′- ATCGGTCGACGCTCTCCC TT/idSp/TGCGACTCCTGCATTAGGAA) using pBR322 as template. Oligos containing 135 thymidylates (5′-AAGGGAGAGCGTCGACCGAT$(T)_{135}$CTTACTG TCATGCCATCCG) was first phosphorylated by T4 PNK (NEB) and then ligated with the 131/151 hybrid in the presence of T4 DNA ligase (NEB) to generate a 151/305 hybrid DNA. After gel purification, the 151/305 hybrid DNA was then annealed with a biotin-tagged primer (5′-biotin-CGGATGGCATGACAGTAAG) to create the final $(dT)_{135}$ gapped DNA. $(dT)_{90}$, $(dT)_{100}$, $(dT)_{165}$ and $(dT)_{200}$ gapped DNA substrates were made with the same procedure as $(dT)_{135}$ DNA preparation, but using oligos with various lengths of $(dT)_n$ (n=90, 100, 165 and 200) (Figure S9). Oligos were purchased from Gene Link (oligos containing $(dT)_{165}$ and $(dT)_{200}$), Integrated DNA Technologies (the primer with one abasic site and oligos containing $(dT)_{90}$, $(dT)_{100}$ and $(dT)_{135}$) and Bio Basic Inc. (digoxigenin-labeled primers). For smFRET experiments, the surface-anchored hybrid DNA substrates were prepared by annealing a 5′-Cy5 and 3′-biotin (5′-Cy5/GCCTCGCTGCCGTCGCCA/bio-3′) double-labeled oligo and a 3′-Cy3-labeled oligo containing various numbers of thymidylate at 3′ overhang (5′-TGGCGACGGCaGCGAGGC$(dT)_n$/Cy3-3′) in the buffer containing 20 mM Tris and 0.5 M NaCl at pH = 8.

Proteins and buffers. mRAD51, mS5S1, $mS5^{FL/AA}S1$, SpRad51, SpS5S1, and SpS5S1C were purified as previously described(2-5). All mouse experiments were carried out with buffer containing 30 mM Tris, 2.5 mM magnesium chloride and 150 mM potassium chloride at pH=7.5. Fission yeast reactions were performed with buffer containing 25 mM Tris, 3 mM magnesium acetate and 150 mM potassium chloride at pH=7.5. ATP and AMPPNP were purchased from Sigma-Aldrich.

Detailed experimental procedures of single-molecule tethered particle motion (TPM) assembly experiment. For S5S1 titration experiments (Figure 1 and 4), 0.8 μM mouse RAD51 (or 0.3 μM fission yeast Rad51) was pre-incubated with the indicated concentrations of mouse S5S1 (or fission yeast S5S1) in corresponding buffers to form complexes at 37°C for 10-15 min. The RAD51-S5S1-ATP mixture

was cooled down to the room temperature and flowed into the reaction chamber containing bead-tagged DNA substrates. For nucleation unit determination, mRAD51 (or SpRad51) at different concentrations (Figure 2A & S9B) or 0.4-1.0 μM mRAD51 plus 1.6 or 2.0 μM (2-fold excess) mS5S1 (Figure 2B) were pre-incubated in corresponding buffers for 10-15 min at 37^{o}C before experiments. For binding preference determination (Figure 2C & S9B), 0.8 μM mRAD51, 0.8 μM mRAD51 plus 1.6 μM mS5S1 or 0.5 μM SpRad51 in corresponding reaction buffers were incubated for 10-15 min at 37^{o}C.

Single-molecule TPM disassembly experiment and data analysis. In disassembly experiments, we used silanized glass slide to avoid extensive surface-protein interaction. To prepare the silanized surface, the glass slides were sequentially sonicated in 2 M KOH for 5 min, 99 % ethanol for 15-20 min and ddH_2O for 15-20 min. After these sonication steps, slides were rinsed with ddH_2O and dried with N_2 gas. Glass slides were then functionalized in a solution containing 1,7-dichloro-octamethytetrasiloxane (Sigma-Aldrich) in 99 % ethanol in the dark overnight at room temperature. Slides were then rinsed with 99 % ethanol and ddH_2O alternatively and dried with N_2. Surface-bound $(dT)_{135}$ gapped DNA substrates were pre-incubated with mixtures of either 0.8 μM mRAD51-2 mM ATP or 0.8 μM SpRad51-2 mM ATP to form nucleoprotein filaments. After 5-10 min incubation, free mRAD51 or SpRad51 were removed with reaction buffer containing no mRAD51/SpRad51. The extensive wash used in our experiments didn't lead to disruption of protein filaments. For disassembly experiments involving S5S1, we added pre-incubated mixtures including 0.3 μM mRAD51 (or SpRad51), indicated amounts of mS5S1 (or SpS5S1), 2 mM ATP and ATP regeneration system (1 mM phosphoenolpyruvate and 4 units/ml pyruvate kinase) into reaction chambers and incubated for 10-15 min to form S5S1-coated Rad51-ssDNA filaments. After 10-15 min incubation, free Rad51 were removed by reaction buffer containing S5S1, ATP, and ATP regeneration system but without mRAD51/SpRad51. Tethers with BM ranging from 35 to 80 nm were scored as Rad51 nucleoprotein filaments (Figure S1).

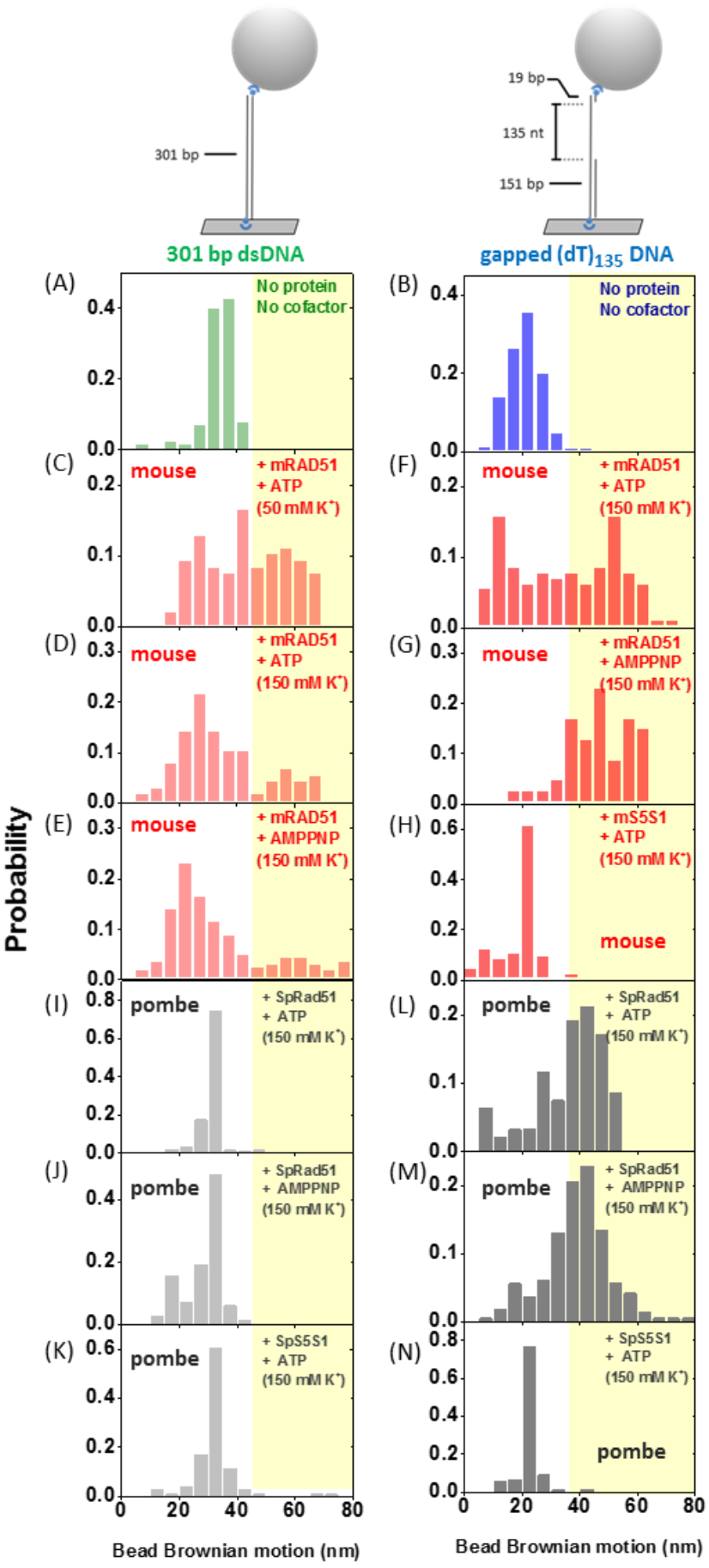
301 bp
19 bp
135 nt
151 bp
301 bp dsDNA
gapped (dT)135 DNA
(A)
No protein
No cofactor
(B)
No protein
No cofactor
(C)
mouse
+ mRAD51
+ ATP
(50 mM K+)
(F)
mouse
+ mRAD51
+ ATP
(150 mM K+)
(D)
mouse
+ mRAD51
+ ATP
(150 mM K+)
(G)
mouse
+ mRAD51
+ AMPPNP
(150 mM K+)
(E)
mouse
+ mRAD51
+ AMPPNP
(150 mM K+)
(H)
+ mS5S1
+ ATP
(150 mM K+)
mouse
(I)
pombe
+ SpRad51
+ ATP
(150 mM K+)
(L)
pombe
+ SpRad51
+ ATP
(150 mM K+)
(J)
pombe
+ SpRad51
+ AMPPNP
(150 mM K+)
(M)
pombe
+ SpRad51
+ AMPPNP
(150 mM K+)
(K)
pombe
+ SpS5S1
+ ATP
(150 mM K+)
(N)
+ SpS5S1
+ ATP
(150 mM K+)
pombe
Probability
Bead Brownian motion (nm)
Bead Brownian motion (nm)

Figure S1. Bead BM histograms of RAD51/S5S1 assembly on either 301 bp dsDNA or $(dT)_{135}$ gapped DNA. Brownian motion (BM) amplitudes of **(A)** bare 301 bp dsDNA and **(B)** bare $(dT)_{135}$ gap DNA substrates are about 35.2±3.77 and 21.3± 5.78 nm, respectively. BM higher than 35 nm (for $(dT)_{135}$ gapped DNA experiments) or 45 nm (for 301 bp dsDNA experiments) is considered to be extended by recombinases (yellow shaded region). Mouse mRAD51 binds to duplex DNA substrates at low salt **(C)**, but shows a reduced dsDNA affinity at higher (150 mM) KCl concentration in the presence of either **(D)** ATP **or (E) AMPPNP** . In contrast, mouse mRAD51 assembles efficiently on the $(dT)_{135}$ gapped DNA under ATP **(F)**, and it assembles much faster under AMPPNP **(G)**. mS5S1 didn't alter BM **(H)**, consistent with the biochemical characterization that mS5S1 has no ssDNA affinity. For pombe, SpRad51 has negligible dsDNA affinity and caused no increase in bead BM in either ATP **(I) or AMPPNP (J)**. **(L-M)** In contrast, SpRad51 preferentially assembled onto ssDNA region of $(dT)_{135}$ gapped DNA at higher KCl concentration in the presence of two cofactors, resulting in the increase of bead BM. Even though SpS5S1 can bind dsDNA and ssDNA, its binding does not change the BM of both substrates **(K and N)**. All assembly experiments were performed at 2 mM ATP or AMPPNP and collected after 5 minutes of protein introduction.

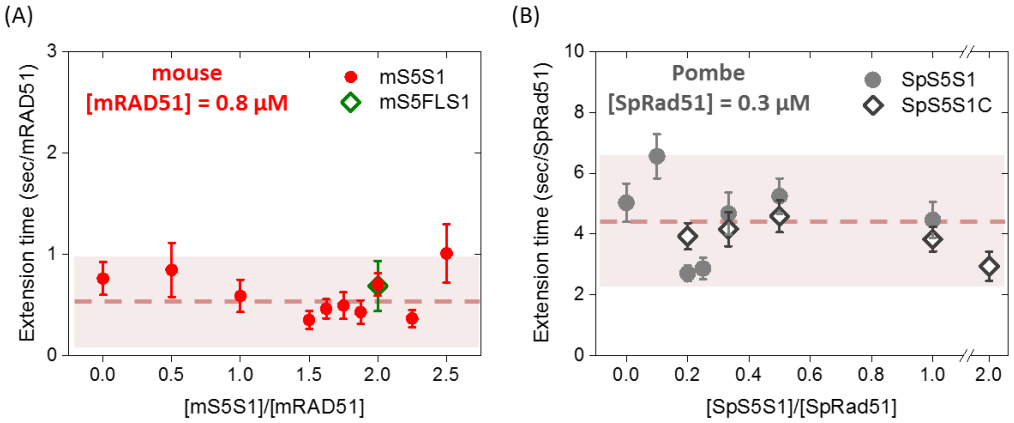

Figure S2. S5S1 shows negligible effects on Rad51 extension time in both two species. At fixed Rad51 concentrations (0.8 µM for mRAD51 and 0.3 µM for SpRad51), Rad51 extension times of both **(A)** mouse and **(B)** pombe display no apparent dependence on S5S1 concentration. Dash line is the mean of all measurements, and the shaded region span two standard deviations. Error bar is one standard error of the mean. Extension times of each concentration ratios are determined as the mean from at least 5 independent experiments.

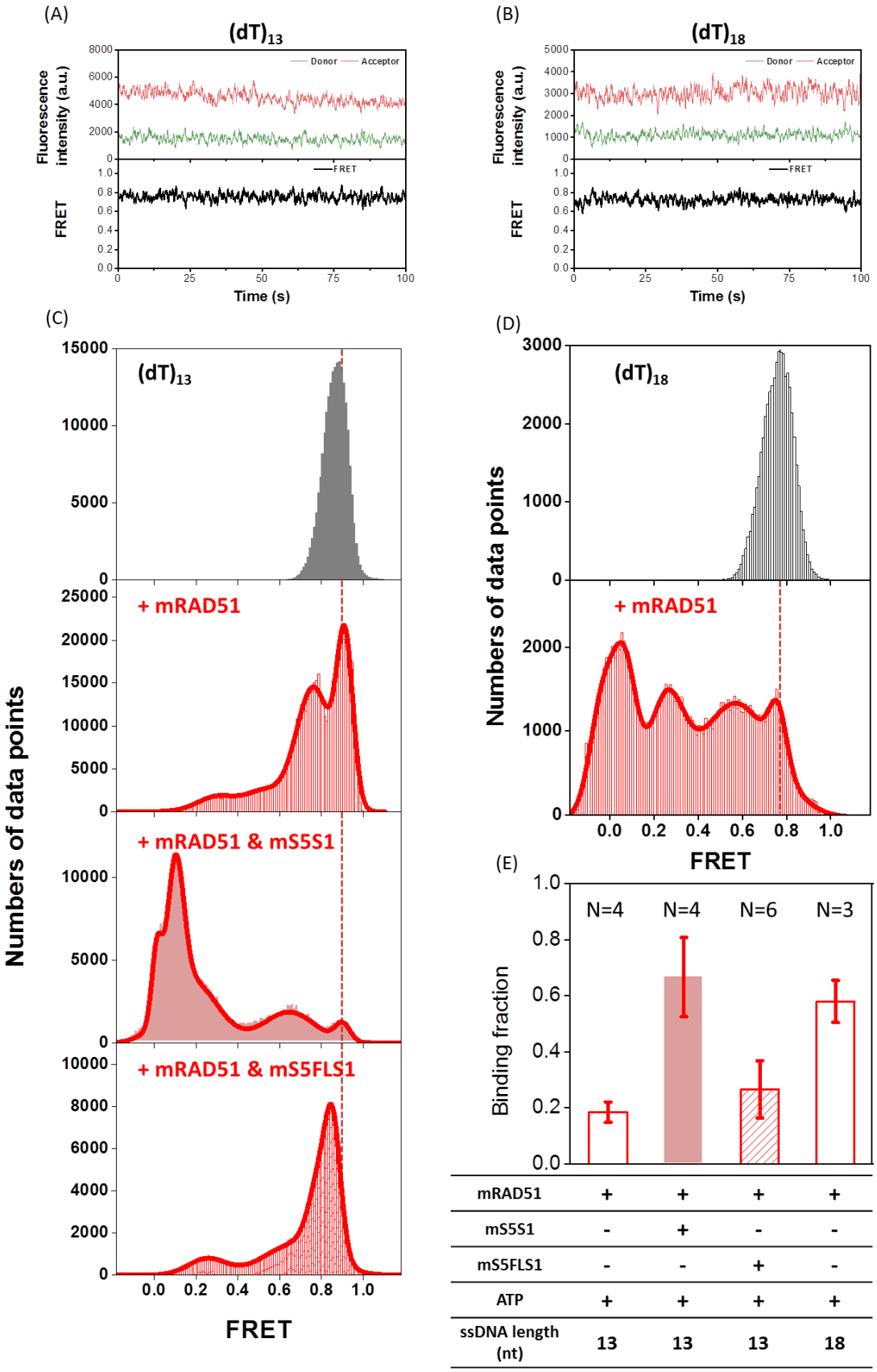

mRAD51	+	+	+	+
mS5S1	-	+	-	-
mS5FLS1	-	-	+	-
ATP	+	+	+	+
ssDNA length (nt)	13	13	13	18

Figure S3. FRET histograms and binding fraction of mRAD51 assembling under different conditions. (A) & **(B)** In the absence of proteins, DNA molecules exist in

the high FRET state owing to the flexibility of ssDNA region. Both bare DNA substrates of different ssDNA lengths exhibit a high FRET state (E ~ 0.7-0.8). **(C)** FRET histograms of $(dT)_{13}$ DNA substrate in the absence of mRAD51 (top panel); in the presence of mRAD51 (second panel from top); in the presence of mRAD51 and mS5S1 mixture (third panel from top) or in the presence of mRAD51 and $mS5^{FL}S1$ mixture (bottom panel). **(D)** FRET histograms of $(dT)_{18}$ DNA substrate in the absence (upper) or in the presence (lower) of mRAD51. **(E)** Binding fraction of mRAD51 assembling on (dT)13 DNA substrate increases in the presence of mS5S1**.** At this $(dT)_{13}$ substrate, binding fraction of mRAD51-only is 18.5±3.62%, and that of mRAD51 and mS5S1 mixture is 66.6±14.0%. mRAD51 and $mS5^{FL}S1$ mixture gives a binding fraction of 26.6±10.2%, which is similar to that of mRAD51-only case. mRAD51 concentration is 1.0 μM, mS5S1 and $mS5^{FL}S1$ concentration are 2.0 μM. At longer $(dT)_{18}$ DNA substrates, the binding fraction is 58.0±7.51%. *N* indicates the number of independent experiments. Dash lines were drawn for guidance purpose.

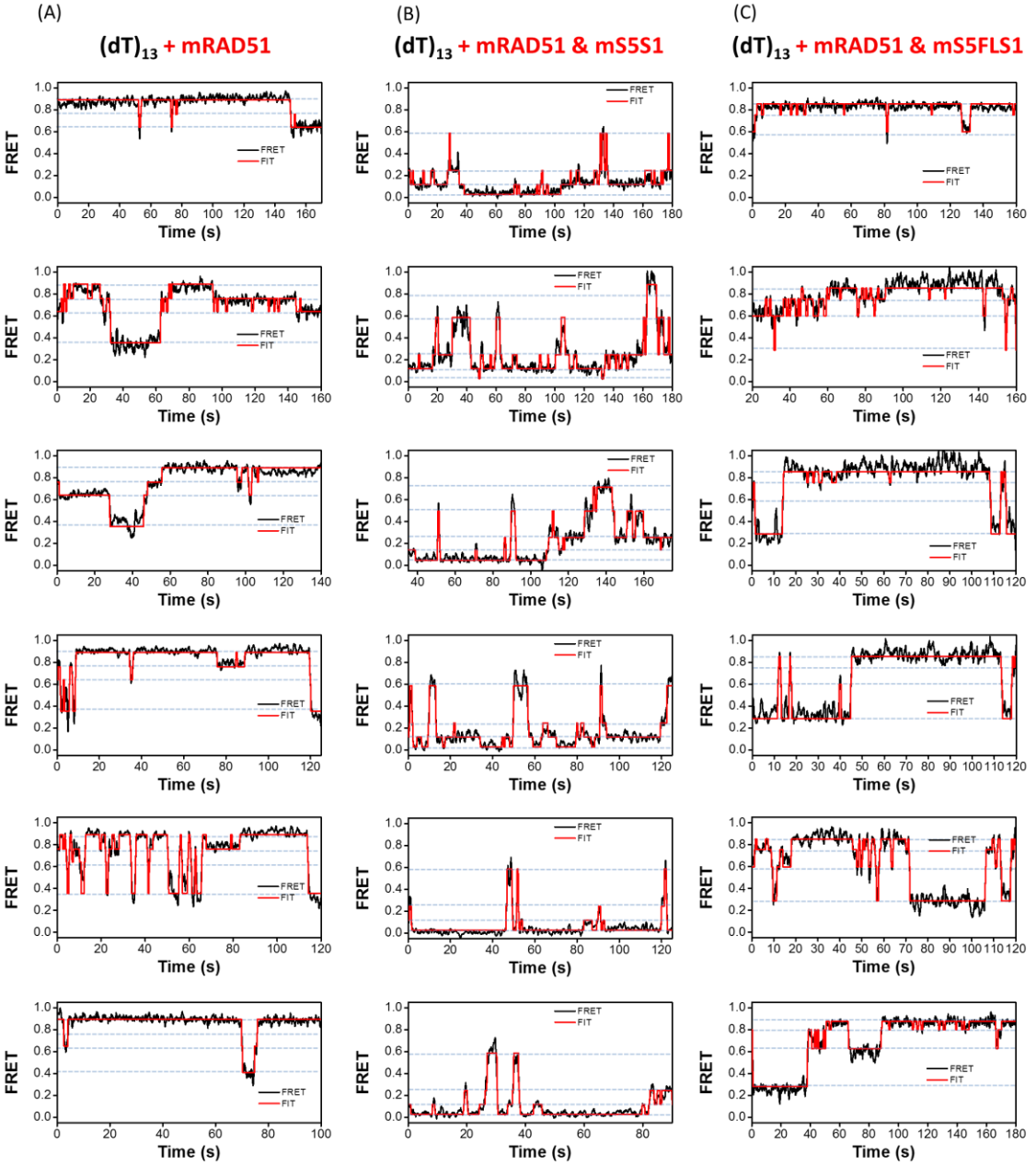
(A)
(dT)13 + mRAD51
(B)
(dT)13 + mRAD51 & mS5S1
(C)
(dT)13 + mRAD51 & mS5FLS1
(D)
(dT)18 + mRAD51
FRET
Time (s)
FRET
FIT

Figure S4. Representative FRET time traces of mRAD51 assembling under three different conditions: (A) on $(dT)_{13}$ substrate; **(B)** on $(dT)_{13}$ substrate in the presence of 2 μM mS5S1; **(C)** on $(dT)_{13}$ substrate in the presence of 2 μM $mS5^{FL}S1$; **(D)** on $(dT)_{18}$ substrate.

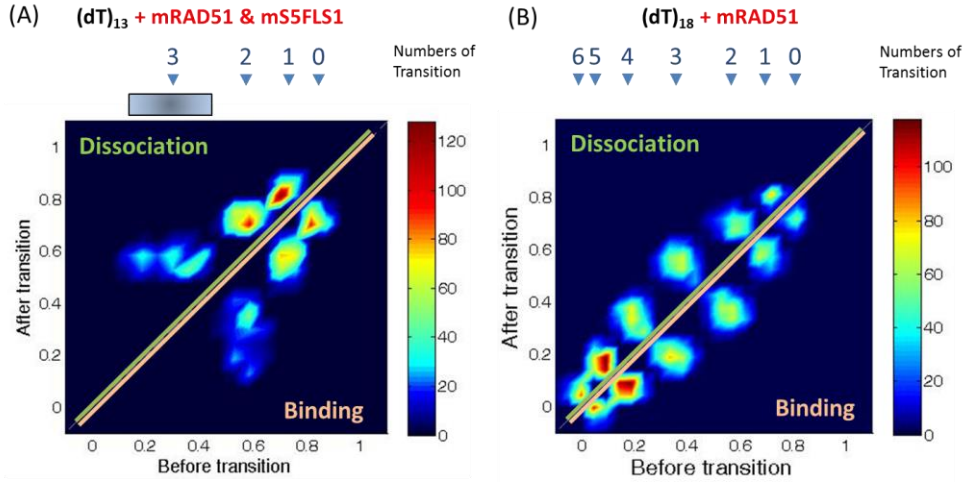

Figure S5. Transition density plot of mRAD51 assembly on $(dT)_{13}$ substrate in the presence of $mS5^{FL}S1$ and $(dT)_{18}$ substrate in the absence of mS5S1. (A) Adding $mS5^{FL}S1$ mutant gave similar transition with RAD51-only case. **(B)** TDP of mRAD51 assembly on $(dT)_{18}$ substrate clearly identifies 7 states, corresponding to zero, one to six mRAD51 monomer(s) binding.

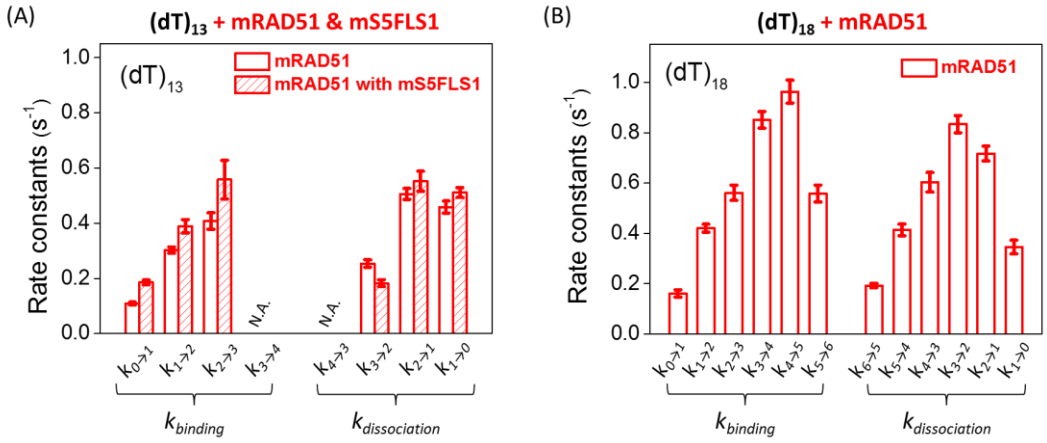

Figure S6. Rate constants of mRAD51 assembling on (A) on $(dT)_{13}$ substrate in the presence of $mS5^{FL}S1$ and (B) $(dT)_{18}$ DNA substrate in the absence of mS5S1.

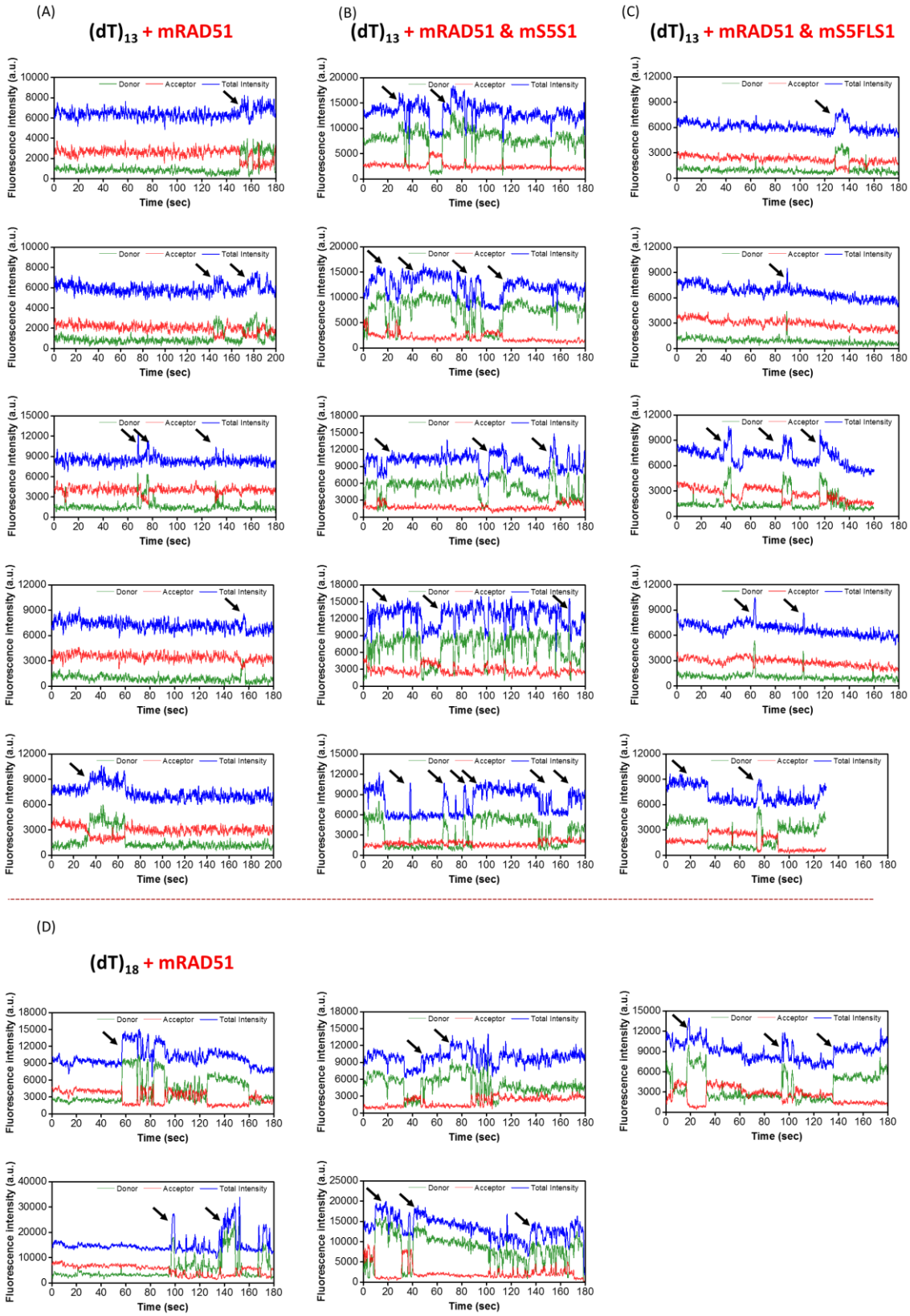

Figure S7. Protein-induced fluorescence enhancement (PIFE) effects are more apparent as mRAD51 assembles on $(dT)_{13}$ substrate in the presence of mS5S1 or on longer $(dT)_{18}$ substrate. Representative fluorescence intensity time traces of

mRAD51 assembling under three different conditions: **(A)** on $(dT)_{13}$ substrate; **(B)** on $(dT)_{13}$ substrate in the presence of 2 μM mS5S1; **(C)** on $(dT)_{13}$ substrate in the presence of 2 μM mS5^{FL}S1; **(D)** on $(dT)_{18}$ substrate. Black arrows indicate the increase in total fluorescence intensity owing to the Cy3 PIFE effect.

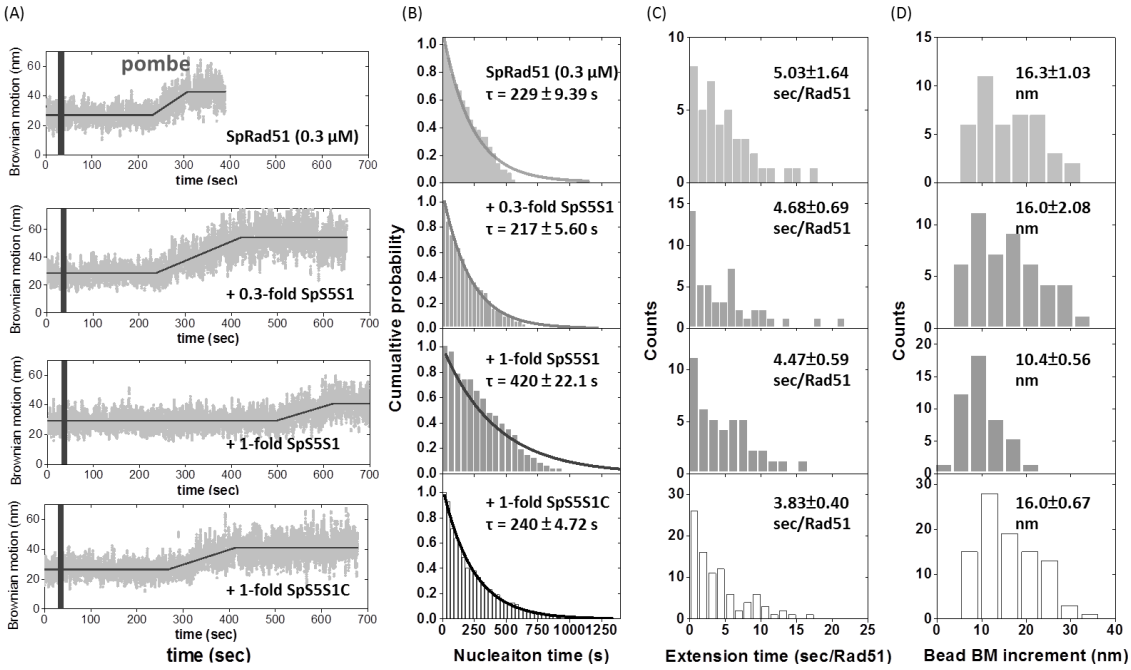

Figure S8. SpRad51 nucleoprotein filament assembly experiments. (A) Representative bead BM time-courses of SpRad51 (0.3 μM) assembly on $(dT)_{135}$ DNA substrates without SpS5S1 (top), with 0.3-fold (0.1 μM) SpS5S1 (middle top), with 0.3 μM SpS5S1 (middle bottom) or with 0.3 μM SpS5S1C mutant (bottom). Gray bars correspond to the deadtime when recombinase mixtures with 2 mM ATP were introduced. Histograms of nucleation time **(B)**, mean extension time (second/Rad51) **(D)** and bead BM increment **(E)** of SpRad51 assembling. All experiments were carried out at 2 mM ATP. Error bar of nucleation rate was the standard deviation of the mean by bootstrapping 5000 times, and error bar of extension time and bean BM increment is one SEM.

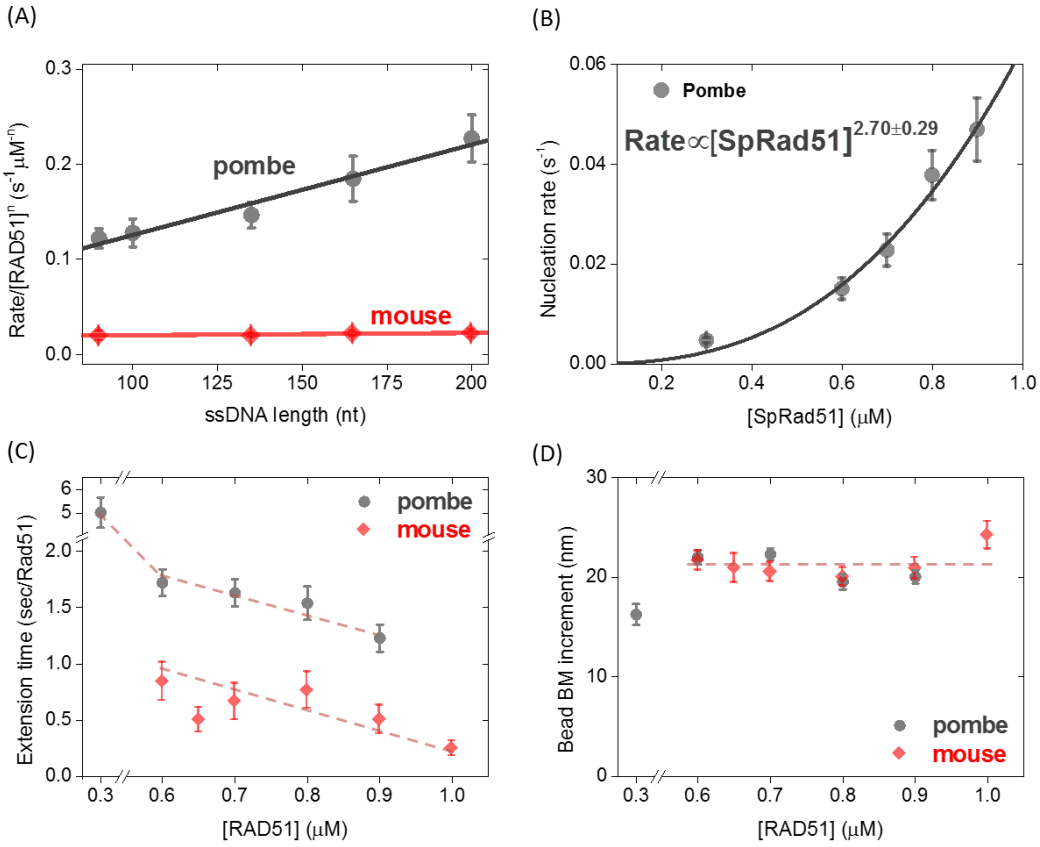

Figure S9. Kinetic parameters of SpRad51 nucleoprotein filament assembly and comparison with mRAD51. (A) ssDNA length dependence of pombe and mouse Rad51 obtained from TPM experiments. Nucleation rates are fitted by a $Rate/[RAD51]^n = k_{ssDNA}*L_{ssDNA}+k_{junction}$. Compared to mRAD51, SpRad51 shows a strong tendency to form nuclei on the ssDNA tail of the resected DNA. **(B)** SpRad51 concentration dependence of filament nucleation obtained by TPM experiments. Power-law fitting returns the nucleation unit of n=2.70±0.29 for SpRad51. **(C)** Extension time obtained from the slope of the BM time-courses and was expressed by the time required to add one Rad51 onto the filament. SpRad51 extends slower than mRAD51. **(D)** Similar bead BM increments between mRAD51 and SpRad51 assembly indicate the similar nucleoprotein filament structure of these two recombinases. At low SpRad51 concentration (0.3 μM), the equilibrium filament length is shorter. Dashed lines are drawn for guidance purpose. Error bar is one standard error of the mean.

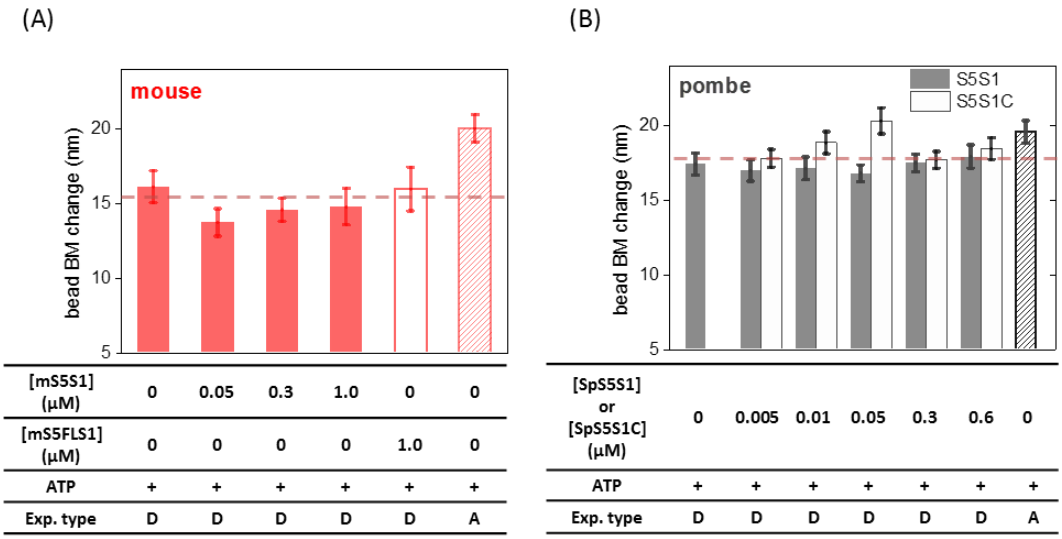

Figure S10. Filament disassembly of mRAD51 and SpRad51 filaments. (A) Bead BM decreases in TPM disassembly experiments of mRAD51 with either S5S1 or $S5^{FL}S1$ are all smaller than BM increment in mRAD51 assembly experiment (the last column in dashed bar) as $(dT)_{135}$ gapped DNA substrate was used in both assembly and disassembly experiments, implicating that not all mRAD51 dissociated from the gapped DNA substrates. **(B)** Compared to mRAD51 disassembly, SpRad51 most entirely dissociated from DNA. Both wild-type SpS5S1 (gray bars) and SpS5S1C mutants (light bars) showed a similar pattern. 0.8 μM of mRAD51 and SpRad51, a specified amount of S5S1 and ATP were used in the preparation of the filament before the disassembly was initiated. Dashed lines are drawn for guidance purpose (A: assembly experiment; D: disassembly experiment). Error bar is one standard error of the mean.

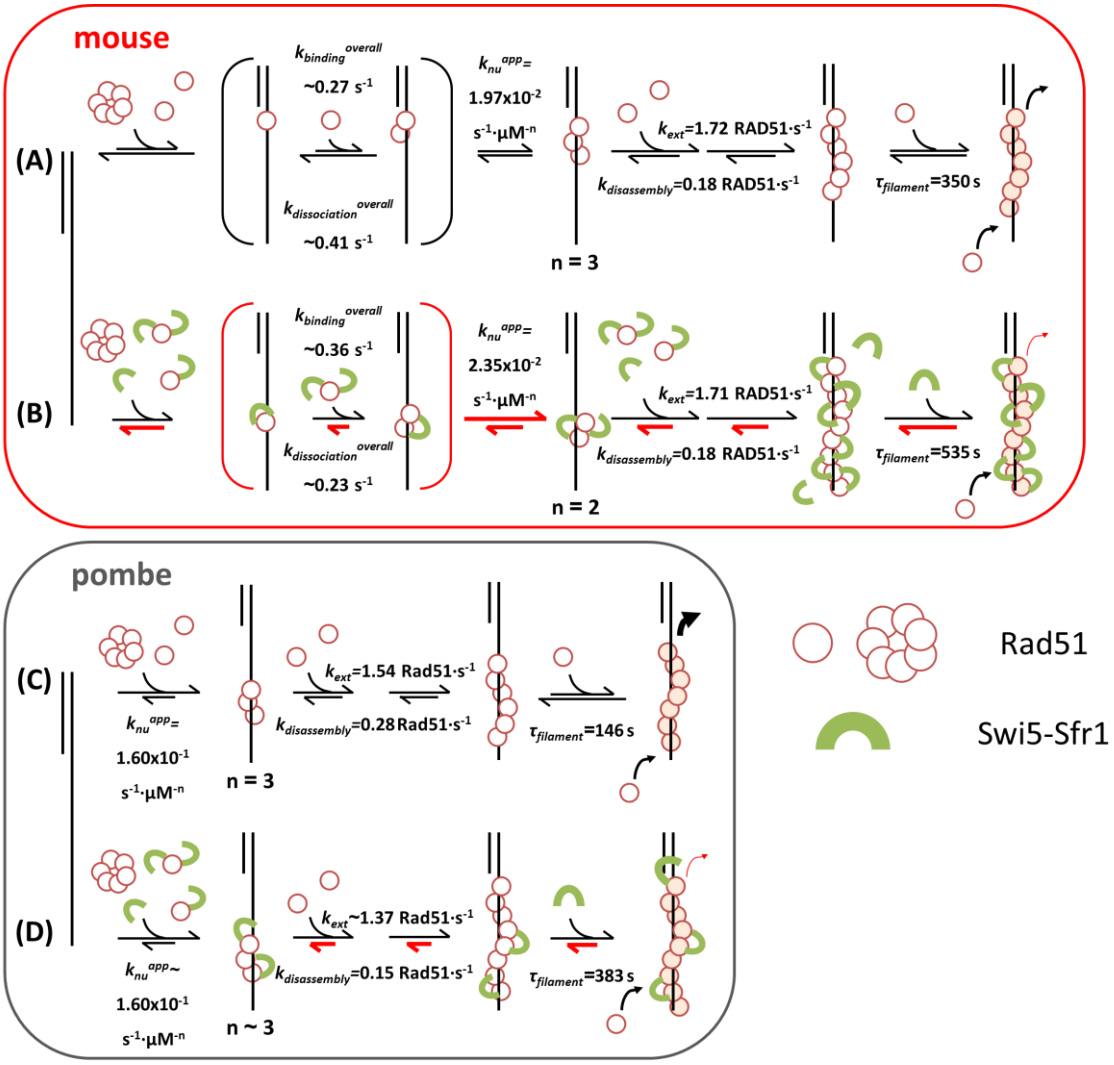

Figure S11. Kinetic parameters for S5S1-regulated Rad51 presynaptic filament formation obtained collectively from smFRET and TPM experiments. (A) Mouse RAD51 forms a stable nucleating cluster made of 3 monomers and extends on ssDNA as a monomer. **(B)** In the presence of mS5S1, mRAD51 interacts with S5S1 to form complex in solution. mS5S1 stimulates mRAD51 nucleation step by reducing mRAD51 nucleation unit from 3 to 2 monomers, stabilizing mRAD51 nucleating clusters and increasing mRAD51 ssDNA affinity. Also, mS5S1 prevents mRAD51 nucleoprotein filament disassembly. **(C & D)** Fission yeast SpS5S1 showed no stimulation on SpRad51 nucleation. Compared to mRAD51, SpRad51 displays a much higher nucleation rate owing to greater k_{ssDNA}. 3 SpRad51 monomers are required for stable nucleating cluster formation. SpRad51 filament is prone to disassembly compared to mRAD51. SpS5S1 efficiently prevents the disassembly of SpRad51 filament, and only small amounts of SpS5S1 is sufficient for stabilization. Different regulation strategies among species allow S5S1 to stabilize Rad51 filament efficiently. Red half-arrows indicate the kinetic steps affected by the S5S1.

Table S1. Summary of *apparent* nucleation rate constants of mRAD51 and mRAD51-S5S1 assembly on various gapped DNA substrates from Figure 2C. Error bar is the standard error of the fits.

	mRAD51	mRAD51-S5S1
k_{ssDNA}^{app} ($s^{-1} \cdot nt^{-1}$)	$(1.40 \pm 0.52) \times 10^{-5}$	$(8.95 \pm 1.93) \times 10^{-5}$
$k_{junction}^{app}$ (s^{-1})	$(9.54 \pm 0.70) \times 10^{-3}$	$(4.11 \pm 2.96) \times 10^{-3}$

Table S2. Summary of nucleation rate constants of mRAD51 and SpRad51 assembly on various gapped DNA substrates in Figure S9A. Error bar is the standard error of the fits.

	mRAD51	SpRad51
k_{ssDNA} ($s^{-1} \cdot nt^{-1} \cdot \mu M^{-n}$)	$(2.41 \pm 0.90) \times 10^{-5}$	$(9.50 \pm 0.99) \times 10^{-4}$
$k_{junction}$ ($s^{-1} \cdot \mu M^{-n}$)	$(1.64 \pm 0.14) \times 10^{-2}$	$(3.07 \pm 1.43) \times 10^{-2}$

Table S3. Summary of data in Figure 1 & S2A.

Initial [mRAD51] (μM)	**[mS5S1]/ [mRAD51]**	**SWI5-SFR1 type**	**Cofactor type**	**Nucleation rate (s^{-1})**	**Extension time (sec/RAD51)**	**Bead BM increment (nm)**	***n*** **(Numbers of molecules)**
0.8	0	--	ATP	$(1.10\pm0.12)*10^{-2}$	0.76±0.16	20.0±0.92	67
	0.5	Wild-type mS5S1		$(1.07\pm0.16)*10^{-2}$	0.85±0.27	24.4±1.45	43
	1			$(1.03\pm0.12)*10^{-2}$	0.59±0.16	26.0±1.35	52
	1.5			$(1.05\pm0.16)*10^{-2}$	0.35±0.09	22.7±1.24	44
	1.625			$(1.02\pm0.18)*10^{-2}$	0.46±0.09	23.5±1.36	48
	1.75			$(1.05\pm0.10)*10^{-2}$	0.49±0.13	26.5±2.26	51
	1.875			$(1.24\pm0.14)*10^{-2}$	0.43±0.11	24.6±1.32	59
	2			$(1.43\pm0.15)*10^{-2}$	0.70±0.11	24.4±0.97	76
	2.25			$(1.44\pm0.18)*10^{-2}$	0.37±0.08	25.2±1.21	54
	2.5			$(1.49\pm0.24)*10^{-2}$	1.01±0.29	25.2±1.79	30
	2	$mS5^{FL/AA}S1$ mutant		$(1.02\pm0.12)*10^{-2}$	0.67±0.24	22.5±1.39	39
	0	--	AMPPNP	$(1.73\pm0.22)*10^{-2}$	0.37±0.07	27.1±1.46	45

Table S4. Summary of data in Figure 2A, 2B, S9C & S9D.

Initial [mRAD51] (μM)	**Initial [mS5S1] (μM)**	**SWI5-SFR1 type**	**Cofactor type**	**Nucleation rate (s^{-1})**	**Extension time (sec/RAD51)**	**Bead BM increment (nm)**	***n*** **(Numbers of molecules)**
No mS5S1							
0.6	0	--	ATP	$(7.47\pm0.70)*10^{-3}$	0.80±0.20	21.7±0.97	92
0.65				$(8.54\pm1.56)*10^{-3}$	0.50±0.11	20.9±1.45	44
0.7				$(9.65\pm1.16)*10^{-3}$	0.66±0.16	20.5±0.97	60
0.8				$(1.10\pm0.12)*10^{-2}$	0.76±0.16	20.0±0.92	67
0.9				$(1.34\pm0.19)*10^{-2}$	0.50±0.13	20.9±1.08	41
1.0				$(2.36\pm0.35)*10^{-2}$	0.24±0.07	24.2±1.38	39
With mS5S1							
0.4	1.6	Wild-type mS5S1	ATP	$(5.34\pm1.15)*10^{-3}$	0.80±0.20	21.1±1.57	29
0.5				$(7.59\pm1.05)*10^{-3}$	0.49±0.12	25.7±1.79	37
0.6				$(1.13\pm0.15)*10^{-2}$	0.62±0.17	24.7±1.63	33
0.7				$(1.25\pm0.16)*10^{-2}$	0.34±0.11	27.6±1.92	31
0.8				$(1.43\pm0.15)*10^{-2}$	0.70±0.11	24.4±0.97	76
1.0	2.0			$(2.44\pm0.36)*10^{-2}$	0.69±0.15	25.7±1.74	37
0.7	1.6	$mS5^{FL/AA}S1$ mutant		$(9.95\pm1.35)*10^{-3}$	0.82±0.20	21.0±1.17	52
0.8				$(1.02\pm0.12)*10^{-2}$	0.67±0.24	22.5±1.39	39

Table S5. Summary of data in Figure 2C.

Initial [mRAD51] (μM)	**Initial [mS5S1] (μM)**	**SWI5-SFR1 type**	**Cofactor type**	**ssDNA length (nt)**	**Nucleation rate (s^{-1})**	***n*** **(Numbers of molecules)**
No mS5S1						
0.8	0	--	ATP	90	$(1.09\pm0.28)*10^{-2}$	31
				135	$(1.10\pm0.12)*10^{-2}$	67
				165	$(1.22\pm0.17)*10^{-2}$	33
				200	$(1.23\pm0.22)*10^{-2}$	42
With mS5S1						
0.8	1.6	Wild-type mS5S1	ATP	90	$(1.32\pm0.28)*10^{-2}$	32
				135	$(1.43\pm0.15)*10^{-2}$	76
				165	$(1.94\pm0.42)*10^{-2}$	35
				200	$(2.26\pm0.22)*10^{-2}$	36

Table S6. Summary of data in Figure 3F, S3E & S6.

Initial [mRAD51] (μM)	Initial [mS5S1] (μM)	SWI5-SFR1 type	Cofactor type	Binding rate (s^{-1})		Dissociation rate (s^{-1})		Binding fraction (%)	n (Numbers of molecules)
$(dT)_{13}$									
1.0	0	--	ATP	$k_{0\to1}$	0.11±0.01	$k_{1\to0}$	0.46±0.02	18.5±3.62	315
				$k_{1\to2}$	0.30±0.01	$k_{2\to1}$	0.51±0.02		
				$k_{2\to3}$	0.41±0.03	$k_{3\to2}$	0.25±0.01		
				$k_{3\to4}$	--	$k_{4\to3}$	--		
	2.0	Wild-type mS5S1		$k_{0\to1}$	0.15±0.01	$k_{1\to0}$	0.15±0.01	66.6±14.0	472
				$k_{1\to2}$	0.33±0.01	$k_{2\to1}$	0.36±0.02		
				$k_{2\to3}$	0.52±0.02	$k_{3\to2}$	0.23±0.01		
				$k_{3\to4}$	0.44±0.02	$k_{4\to3}$	0.18±0.01		
	2.0	$mS5^{FL/AA}S1$ mutant		$k_{0\to1}$	0.17±0.01	$k_{1\to0}$	0.48±0.02	25.0±8.51	120
				$k_{1\to2}$	0.38±0.02	$k_{2\to1}$	0.50±0.03		
				$k_{2\to3}$	0.45±0.06	$k_{3\to2}$	0.17±0.01		
				$k_{3\to4}$	--	$k_{4\to3}$	--		

$(dT)_{18}$									
1.0	0	--	ATP	$k_{0\rightarrow1}$	0.16±0.01	$k_{1\rightarrow0}$	0.35±0.03	58.0±7.51	467
				$k_{1\rightarrow2}$	0.42±0.02	$k_{2\rightarrow1}$	0.72±0.03		
				$k_{2\rightarrow3}$	0.56±0.03	$k_{3\rightarrow2}$	0.83±0.03		
				$k_{3\rightarrow4}$	0.85±0.03	$k_{4\rightarrow3}$	0.60±0.04		
				$k_{4\rightarrow5}$	0.96±0.06	$k_{5\rightarrow4}$	0.41±0.02		
				$k_{5\rightarrow6}$	0.56±0.03	$k_{6\rightarrow5}$	0.19±0.01		

Table S7. Summary of data in Figure 4E, 4F, S2B & S8.

Initial [SpRad51] (μM)	[SpS5S1]/ [SpRad51]	Swi5-Sfr1 type	Cofactor type	Nucleation rate (s^{-1})	Extension time (sec/Rad51)	Bead BM increment (nm)	*n* (Numbers of molecules)
0.3	0	--	ATP	$(4.50\pm0.51)*10^{-3}$	5.03±0.64	16.3±1.04	42
	0.1	Wild-type SpS5S1		$(5.05\pm0.59)*10^{-3}$	6.56±0.73	14.8±0.76	68
	0.2			$(4.20\pm0.57)*10^{-3}$	2.70±0.26	16.4±1.01	38
	0.25			$(4.84\pm0.73)*10^{-3}$	2.87±0.34	18.0±1.12	41
	0.33			$(4.91\pm0.62)*10^{-3}$	4.68±0.69	16.0±1.08	48
	0.5			$(3.09\pm0.35)*10^{-3}$	5.25±0.58	13.4±0.80	52
	1			$(2.39\pm0.24)*10^{-3}$	4.47±0.59	10.4±0.56	45
	0.2	SpS5S1C mutant		$(4.74\pm0.60)*10^{-3}$	3.93±0.44	16.0±0.94	50
	0.33			$(4.73\pm0.53)*10^{-3}$	4.16±0.56	14.4±0.57	73
	0.5			$(4.17\pm0.39)*10^{-3}$	4.58±0.52	15.4±0.66	82
	1			$(4.37\pm0.45)*10^{-3}$	3.83±0.40	15.9±0.67	94
	2			$(4.21\pm0.57)*10^{-3}$	2.94±0.48	13.5±0.83	35
	0	--	AMPPNP	$(8.72\pm1.36)*10^{-3}$	2.89±0.70	16.6±0.92	30

Table S8. Summary of data in Figure 5 & S10.

Species	Final [S5S1] (μM)	Swi5-Sfr1 type	Cofactor type	Minimum mean lifetime (sec)	Fraction of un-disassembled filament (%)	Disassembly time (sec/Rad51)	Bead BM decrease (nm)	*n* (Numbers of molecules)
Mouse	0	--	ATP	350±39.3	17.0	5.62±1.35	16.1±1.08	47
	0.05	Wild-type mS5S1		441±51.1	29.5	5.86±1.02	13.7±0.93	44
	0.3			467±35.2	30.5	4.41±0.80	14.5±0.79	83
	1.0			535±49.9	34.1	6.20±1.96	14.7±1.22	44
	0.3	$mS5^{FL/AA}S1$ mutant		393±54.9	20.5	4.86±1.46	18.0±1.51	39
	1.0			364±46.4	22.7	4.59±0.97	15.9±1.48	44
	0	--	AMPPNP	627±43.9	57.9	5.06±1.88	15.6±1.61	56
Fission yeast	0	--	ATP	140±17.9	2.47	3.55±0.44	17.4±0.74	81
	0.005	Wild-type SpS5S1		256±34.6	17.1	6.77±0.72	16.9±0.71	82
	0.01			382±32.6	27.9	6.43±0.61	17.1±0.68	122
	0.05			367±27.1	26.2	6.57±0.54	16.8±0.56	162
	0.3			378±23.4	23.8	6.21±0.57	17.5±0.59	210
	0.6			407±30.1	25.4	6.29±0.78	17.9±0.78	118
	0.005	SpS5S1C mutant		153±16.4	2.91	4.00±0.37	17.8±0.60	95
	0.01			271±28.8	14.7	4.51±0.41	18.8±0.74	75
	0.05			318±35.1	19.8	4.32±0.49	20.3±0.88	75
	0.3			288±23.0	17.1	4.91±0.44	17.7±0.56	123
	0.6			338±33.8	20.0	4.12±0.59	18.4±0.73	70
	0	--	AMPPNP	579±69.8	48.1	11.9±2.79	11.8±1.12	27

Table S9. Summary of data in Figure S9A.

Species	Initial [Rad51] (μM)	Initial [S5S1] (μM)	Swi5-Sfr1 type	Cofactor type	ssDNA length (nt)	Nucleation rate constant ($s^{-1}\cdot\mu M^{-n}$)	*n* (Numbers of molecules)
Mouse	0.8	0	--	ATP	90	$(1.88\pm0.48)*10^{-2}$	31
					135	$(1.89\pm0.21)*10^{-2}$	67
					165	$(2.10\pm0.28)*10^{-2}$	33
					200	$(2.11\pm0.38)*10^{-2}$	42
fission yeast	0.8	0	--	ATP	90	$(1.22\pm0.10)*10^{-1}$	145
					100	$(1.28\pm0.15)*10^{-1}$	49
					135	$(1.47\pm0.14)*10^{-1}$	131
					165	$(1.85\pm0.24)*10^{-1}$	77
					200	$(2.27\pm0.25)*10^{-1}$	81

Table S10. Summary of data in Figure S9B-S9D.

Initial [SpRad51] (μM)	Initial [SpS5S1] (μM)	Swi5-Sfr1 type	Cofactor type	Nucleation rate (s^{-1})	Extension time (sec/Rad51)	Bead BM increment (nm)	*n* (Numbers of molecules)
0.3	0	--	ATP	$(4.50\pm0.51)*10^{-3}$	5.03±0.64	16.3±1.04	42
0.6				$(1.49\pm0.22)*10^{-2}$	1.72±0.12	22.0±0.70	81
0.7				$(2.26\pm0.32)*10^{-2}$	1.63±0.12	22.3±0.61	104
0.8				$(3.77\pm0.49)*10^{-2}$	1.54±0.15	19.5±0.76	81
0.9				$(4.68\pm0.63)*10^{-2}$	1.22±0.12	20.0±0.68	104

SI References

1. Gal J, Schnell R, Szekeres S, & Kalman M (1999) Directional cloning of native PCR products with preformed sticky ends (Autosticky PCR). *Mol Gen Genet* 260(6):569-573.
2. Kuwabara N, *et al.* (2012) Mechanistic Insights into the Activation of Rad51-Mediated Strand Exchange from the Structure of a Recombination Activator, the Swi5-Sfr1 Complex. *Structure* 20(3):440-449.
3. Tsai SP, *et al.* (2012) Rad51 presynaptic filament stabilization function of the mouse Swi5-Sfr1 heterodimeric complex. *Nucleic Acids Res* 40(14):6558-6569.
4. Su GC, *et al.* (2016) Role of the RAD51-SWI5-SFR1 Ensemble in homologous recombination. *Nucleic Acids Res* 44(13):6242-6251.
5. Kuwabara N, *et al.* (2010) Expression, purification and crystallization of Swi5 and the Swi5-Sfr1 complex from fission yeast. *Acta Crystallogr F* 66:1124-1126.